

# SYMMETRY ENERGY AND SECONDARY DECAY: TOWARDS THE RECONSTRUCTION OF PRIMARY FRAGMENTS\*

P. MARINI, M. BOISJOLI, P. WIGG, A. CHBIHI

GANIL, Bd. H. Becquerel, BP 55027 — 14076 CAEN Cedex 05, France

*(Received February 13, 2013)*

The effects of the secondary deexcitation on isotopic distributions, commonly used as an observable to extract information on the symmetry energy, hints at the necessity of reconstructing primary fragments from measured quantities. Preliminary results of data measured in the  $4\pi$  detector INDRA and the VAMOS spectrometer presented here open up the possibility of planning a program on charged particle spectroscopy of exotic nuclei.

DOI:10.5506/APhysPolB.44.581

PACS numbers: 25.75.Gz

## 1. Introduction

Understanding the properties of asymmetric nuclear matter both at normal densities and at densities away from the saturation density has an important impact on the study of the nuclear structure close to the drip lines [1], of astrophysical processes [2] and of heavy ion reaction mechanisms [3].

Isotopic distributions of complex fragments produced in multifragmentation processes at Fermi energies are common observables used to explore the equation of state (EOS) at subsaturation densities. Indeed theoretical predictions [4] suggest that information can be extracted from the isotopic distributions of primary fragments. However, most fragments, produced in excited states, decay to lighter stable isotopes on a typical time scale of  $\sim 10^{-20}$  s [5, 6], before being detected. Model calculations [7, 8] show that isotopic distributions of secondary fragments (after secondary decay) are distorted and their sensitivity to different parametrizations of the EOS is significantly reduced.

In this work, we present a preliminary analysis aimed at the reconstruction of primary fragments produced in semiperipheral collisions.

---

\* Presented at the Zakopane Conference on Nuclear Physics “Extremes of the Nuclear Landscape”, Zakopane, Poland, August 27–September 2, 2012.

## 2. The experiment

$^{40,48}\text{Ca}$  ion beams were accelerated at the GANIL CIME Cyclotron at 35 MeV/nucleon and impinged on isotopically enriched  $^{40,48}\text{Ca}$  targets. Reaction products were detected in the  $4\pi$  INDRA multidetector array [9] coupled with the VAMOS spectrometer [10]. The high isotopic resolution of the VAMOS spectrometer allows charge and mass identification of forward emitted projectile-like fragments, while the high performance  $4\pi$  detector INDRA provides information on all the associated light charged particles, on an event-by-event basis.

An example of the achieved isotopic resolution for  $Z = 18$  is shown in Fig. 1 (left) for the  $^{40}\text{Ca}+^{48}\text{Ca}$ ,  $^{48}\text{Ca}+^{40}\text{Ca}$  and  $^{48}\text{Ca}+^{48}\text{Ca}$  reactions. Isotopes from  $^{32}\text{Ar}$  to  $^{46}\text{Ar}$  are clearly identified with a  $\Delta A/A \simeq 0.5\%$ .

Further details on the experimental set-up can be found in Ref. [11].

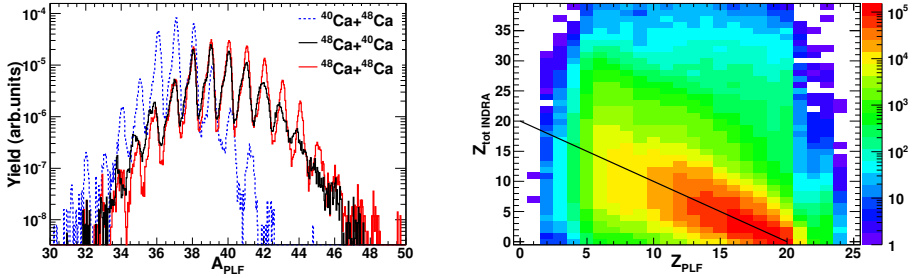


Fig. 1. Left: Mass distribution of  $Z = 18$  PLF detected in the VAMOS spectrometer. Right: Total charge detected in INDRA *versus* charge of the PLF fragment. The line indicate the events with a total detected charge of 20.

## 3. Analysis

The procedure used to reconstruct primary fragment consists in the selection of a PLF and the analysis of particles emitted in coincidence. The results presented here are preliminary and aim to verify the feasibility of the procedure. As a first step, we focused on the  $^{40}\text{Ca}+^{48}\text{Ca}$  peripheral collisions and we investigated the excited states, above the particle emission threshold, of  $^{38}\text{Ar}$  and  $^{35}\text{Cl}$  decaying through S emission. Therefore, only events where a S projectile-like fragment was detected in VAMOS were selected. In each event, light charged particles detected in coincidence in INDRA were accepted requiring their longitudinal velocity relative to the beam velocity to be greater than 50%, in order to remove fragments from pre-equilibrium or quasi-target sources. Later, we will refer to particles passing this selection as particles emitted in coincidence or particles in coincidence.

Fully detected  $^{40}\text{Ca}^*$  quasi-projectile decay events were selected requiring the sum of the fragment charge detected in VAMOS ( $Z_{\text{PLF VAMOS}} = 16$ ) and of the total charge of particles in coincidence ( $Z_{\text{tot INDRA}}$ ) to be  $Z_{\text{tot}} = 20$ , *i.e.*  $Z_{\text{tot}} = Z_{\text{PLF VAMOS}} + Z_{\text{tot INDRA}}$ . In Fig. 1 (right),  $Z_{\text{PLF VAMOS}}$  is plotted *versus*  $Z_{\text{tot INDRA}}$ . The full line indicates Ca fully detected events, *i.e.*  $Z_{\text{tot}} = 20$ . We observe that, thanks to the  $4\pi$  INDRA coverage and its granularity, the majority of the events are fully detected in charge.

Events with 3 particles emitted in coincidence with the S PLF were chosen in the present analysis as a test-case. This selection, combined with the  $Z_{\text{tot}} = 20$  constraint, implies a total charge detected in INDRA  $Z_{\text{tot INDRA}} = 4$ , *i.e.* two  $Z = 1$  and one  $Z = 2$  fragments are emitted in coincidence with the PLF.

A PLF fragment mass  $A_{\text{PLF}} = 34$  was selected in order to obtain the highest available statistics. The analysis of the mass distributions of  $Z = 1$  and  $Z = 2$  particles emitted in coincidence with a  $^{34}\text{S}$  showed that those particles are mainly protons and alphas. Therefore, in the  $^{40}\text{Ca}^*$  reconstruction we considered one  $^{34}\text{S}$ , one  $^4\text{He}$  and two  $^1\text{H}$  fragments. There are four paths through which the primary  $^{40}\text{Ca}^*$  quasi-projectile may decay producing one  $^{34}\text{S}$ , one  $^4\text{He}$  and two  $^1\text{H}$ : a simultaneous break-up in 4 fragments:  $^{40}\text{Ca}^* \rightarrow ^{34}\text{S} + ^4\text{He} + ^1\text{H} + ^1\text{H}$  or a break-up through the formation of an intermediate excited nucleus ( $^{39}\text{K}$ ,  $^{38}\text{Ar}$  and  $^{35}\text{Cl}$ ):

$$^{40}\text{Ca}^* \rightarrow ^{39}\text{K}^* + ^1\text{H} \rightarrow (^{34}\text{S} + ^4\text{He} + ^1\text{H}) + ^1\text{H}, \quad (1)$$

$$^{40}\text{Ca}^* \rightarrow ^{38}\text{Ar}^* + ^1\text{H} + ^1\text{H} \rightarrow (^{34}\text{S} + ^4\text{He}) + ^1\text{H} + ^1\text{H}, \quad (2)$$

$$^{40}\text{Ca}^* \rightarrow ^{35}\text{Cl}^* + ^4\text{He} + ^1\text{H} \rightarrow (^{34}\text{S} + ^1\text{H}) + ^1\text{H} + ^4\text{He}. \quad (3)$$

As an example, we analysed the cases in which the primary  $^{40}\text{Ca}^*$  fragment decays through the formation of the excited  $^{38}\text{Ar}^*$  and  $^{35}\text{Cl}^*$  nuclei. The reconstructed excitation energy of the intermediate fragments was calculated through calorimetry as:  $E^* = \sum_i^{M_{\text{CP}}} K^{\text{CP}}(i) - Q$ , where  $K^{\text{CP}}$  is kinetic energy, in the intermediate fragment center-of-mass, of each particle emitted in  $^{38}\text{Ar}$  and  $^{35}\text{Cl}$  decay, *i.e.* of  $^{34}\text{S}$  and  $^4\text{He}$  for  $^{38}\text{Ar}$  and of  $^{34}\text{S}$  and  $^1\text{H}$  for  $^{35}\text{Cl}$ . The second term is the reaction  $Q$  value. The mass of the intermediate fragment was calculated as the sum of the masses of the charged particles belonging to the considered excited fragment.

In Fig. 2, the excitation energy of the  $^{38}\text{Ar}$  and  $^{35}\text{Cl}$  intermediate fragments is shown. The  $^{38}\text{Ar}$  nucleus presents excited states decaying in  $^{34}\text{S} + ^4\text{He}$  at 9.88 and 14.6 MeV. Similarly, excited states of  $^{35}\text{Cl}$  decaying in  $^{34}\text{S} + ^1\text{H}$  have been observed for excitation energies of 7.09 and 10.0 MeV [12]. Structures are present in the  $^{38}\text{Ar}$  (bottom panel) and  $^{35}\text{Cl}$  (top panel) excitation energy spectra. Two peaks can be observed at the excitation energy

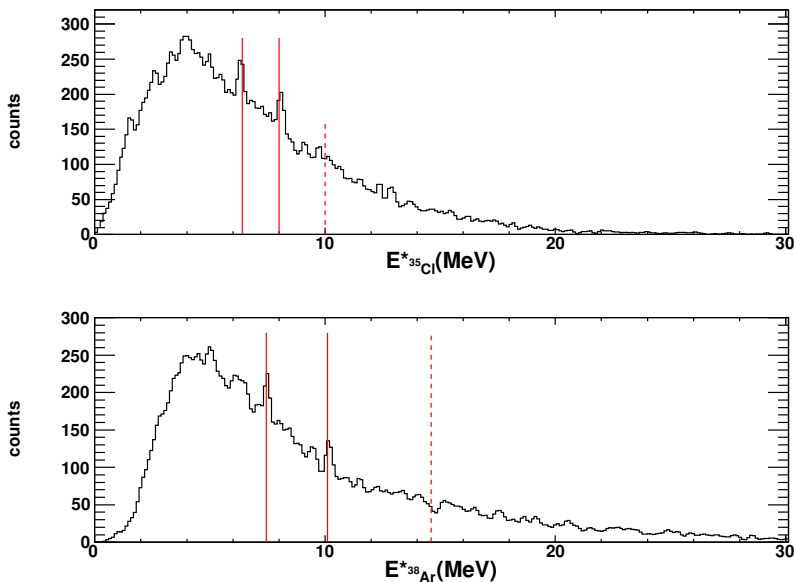


Fig. 2.  $^{35}\text{Cl}$  (top) and  $^{38}\text{Ar}$  (bottom) intermediate fragment excitation energy. Full and dashed lines indicate the peak positions and the expected positions, respectively.

of  $7.4 \pm 0.4$  MeV and  $10.0 \pm 0.3$  MeV and of  $6.2 \pm 0.7$  and  $8.0 \pm 0.6$  MeV, which are consistent with the particle emission threshold and the expected position of the first state of  $^{38}\text{Ar}$  and  $^{35}\text{Cl}$  decaying in  $^{34}\text{S}$ , respectively. We do not observe the expected peaks at 14.6 MeV and 10.0 MeV, probably due to the need of background correction. The observation of these peaks gives us confidence that, with a proper treatment of the background, the spectra can be cleaned up and the peaks unambiguously identified. We should notice that neutrons are not included in the present analysis: the pick up of neutrons from the target (which is neutron rich), followed by their evaporation, could affect the selection of the mass of the excited fragment and might generate spurious peaks in the excitation energy spectra. Other sources of spurious peaks are under investigation. A full calibration of INDRA is required to improve the present analysis, which seems, however, very promising. Also, a background correction with correlation techniques will give us a better insight. This kind of analysis allows one to trace back primary fragments produced in the collisions. Moreover, excited states of exotic nuclei decaying by particle emission could be investigated, giving hints for the planning of more dedicated charged particle spectroscopy experiments to be performed with exotic nuclei.

#### 4. Conclusions

In this work, we presented a procedure to trace back primary fragments exploiting the VAMOS high isotopic resolution and the INDRA granularity and energy resolution. The preliminary results are promising and open up the possibility for a new program on charged particle spectroscopy on exotic nuclei.

#### REFERENCES

- [1] B.A. Brown *et al.*, *Phys. Rev. Lett.* **85**, 5296 (2000).
- [2] J.M. Lattimer *et al.*, *Astrophys. J.* **550**, 426 (2001).
- [3] V. Baran *et al.*, *Phys. Rev.* **410**, 335 (2005) and references therein.
- [4] A. Ono *et al.*, *Phys. Rev.* **C70**, 041604 (2004).
- [5] S. Hudan *et al.*, *Phys. Rev.* **C67**, 064613 (2003).
- [6] V.V. Volkov, *Phys. Rep.* **44**, 93 (1978) and references therein.
- [7] M.B. Tsang *et al.*, *Phys. Rev.* **C64**, 054615 (2001).
- [8] P. Marini *et al.*, [arXiv:1212.3126](#) [nucl-ex].
- [9] J. Pouthas *et al.*, *Nucl. Instrum. Methods Phys. Res. A* **357**, 418 (1995).
- [10] H Savajols *et al.*, *Nucl. Instrum. Methods Phys. Res. B* **204**, 146 (2003).
- [11] P. Marini, Ph.D. Thesis, University of Bologna, 2009.
- [12] P.M. Endt *et al.*, *Nucl. Phys.* **A310**, 1 (1978).